

PROPERTY TEST OF THE Q-FACTOR FOR HIGH-PURITY COPPER AT THE TEMPERATURE OF 20K

A. Iino[#], S. Yamaguchi, SOKENDAI and KEK, Tsukuba, Japan
 K. Endo, TOYAMA Co., Ltd., Kanagawa, Japan

Abstract

A coherent parametric x-ray radiation (PXR) source based on a cryogenic electron linac has been developed by Toyama Co., Ltd, KEK and Nihon University. This accelerator is a C-band normal-conducting compact linac that requires a high Q factor in the accelerating and decelerating structures. To obtain a high Q factor, the accelerating and decelerating structures are operated around 20 K, and are joined by diffusion bonding and are constructed with high-purity 6N8 copper which has very low resistivity in extremely low temperatures. In this study, we report the measurements and calculation of the residual resistance ratio (RRR) for 6N8 copper and oxygen-free copper (Class 1) as well as the Q factor for a pillbox cavity made of 6N8 copper and Class 1. The results of a low-power test of this accelerating structure at low temperature are reported. The Q factor for a 6N8 copper pillbox cavity is not much higher than that of a Class 1 pillbox cavity at low temperatures. Moreover, the Q factor is saturated when RRR is greater than 500.

beam that passes through the PXR-generation is decelerated to 5 MeV (injection energy) in the decelerating structure. The ERL beam energy recovery system is shown in Figure 2. We attempt to achieve high gradient acceleration using this system with high- Q accelerating and decelerating structures, made of 6N8 copper and joined by diffusion bonding, in extremely low temperatures. The parameters of the accelerating structure are shown in Table 1.

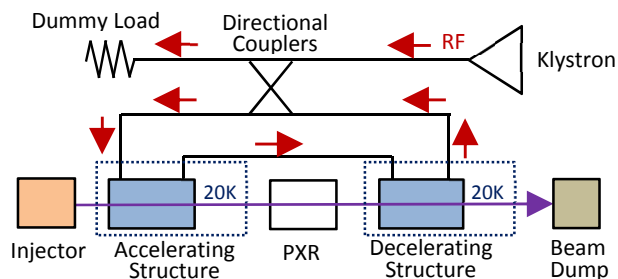


Figure 2: The beam energy recovery system.

INTRODUCTION

The coherent parametric x-ray radiation (PXR) source based on a cryogenic electron linac has been considered for medical applications [1]. However, one major problem in medical applications is the size of the equipment where the PXR source is installed, which is determined by the volume of the radiation shield for the PXR source and linac. Therefore, a normal-conducting compact energy recovery linac (ERL) has been developed for the PXR source to reduce size of the equipment. A schematic of the ERL under development is shown in Figure 1.

To reduce the volume of the radiation shield, the electron

Table 1: Parameters of the Accelerating Structure

Beam Energy	75 MeV
Structure Length	1.3 m
Average E_{acc}	75.5 MV/m
Resonance Frequency	5712 MHz
Working Temperature	20 K
Shunt Impedance	350 M Ω /m
Accelerating Mode	Traveling wave
Phase Advance per Cell	$2\pi/3$

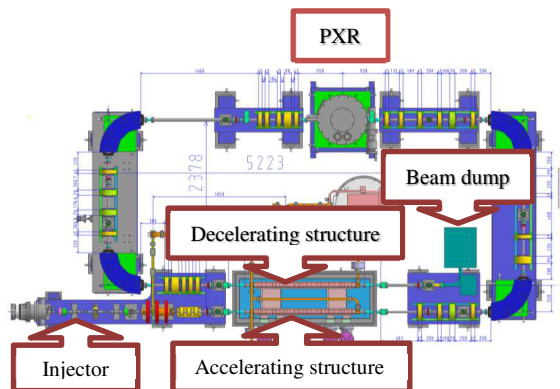


Figure 1: Schematic of the ERL under development.

CALCULATION OF RRR AND Q_0

Calculation of RRR

The relation between the residual resistance ratio (RRR) and the Q factor Q_0 is calculated using the following procedure. First, we calculated the DC conductivity (σ), DC resistivity (ρ), and mean free path (ℓ) from extremely low temperatures to room temperature (20 K to 300 K) using the Wiedemann-Franz law for the thermal conductivity of high-purity copper provided by National Institute of Standards and Technology (NIST). Then, we calculated the surface resistance (R_s), which has a relation to σ , using the theoretical equation in consideration of the anomalous skin effect in the diffusion reflection model and calculated Q_0 [2].

This calculated values of R_s are consistent with the experimental values in range of σ corresponding to the temperature range from 20 K to 300 K [3]. The relations between σ and R_s , which we calculated using this theoretical equation at frequencies of 2856 MHz, 5712 MHz, 8568 MHz, and 11424 MHz, are shown in Figure 3. When $\sigma^{1/2}$ is 40,000, R_s is normalized to be 1 in Figure 3. Furthermore, RRR is proportional to σ at extremely low temperatures,

$$RRR = \frac{\rho(300K)}{\rho(4K)} = \frac{\sigma(4K)}{\sigma(300K)}. \quad (1)$$

As shown in Figure 3, when RRR is above 500, $1/R_s$ becomes saturated at all frequencies.

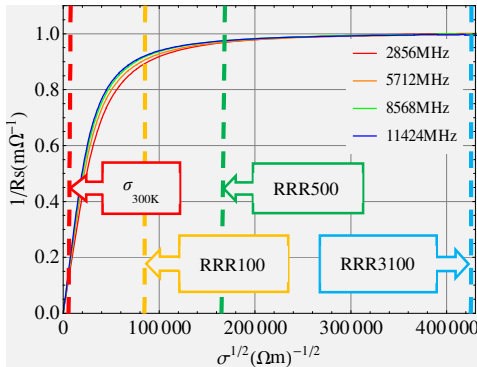


Figure 3: Relation between the surface impedance and DC conductivity of copper.

Calculation of Q_0

The Q_0 value of the TM_{010} pillbox cavity is calculated by

$$Q_0 = \frac{\omega W}{P} = \frac{\omega \mu_0}{2R_s} \frac{rL}{(L+r)}. \quad (2)$$

Here, ω is the angular frequency, μ_0 is the permeability, r is the radius of the cavity, and L is the length of the cavity. Based on equations (1) and (2) and Figure 3, the calculation results for the relation between $Q_0(20K)/Q_0(300K)$ and RRR at 2856 MHz, 5712 MHz, 8568 MHz, and 11424 MHz is shown in Figure 4. The cavity has a radius (r) of 40.176 mm and length (L) of 100 mm. As shown in Figure 4, when RRR is above 500, $Q_0(20K)/Q_0(300K)$ becomes approximately constant, and $Q_0(20K)$ is 5.3 times higher than $Q_0(300K)$ in the C-band frequency. From this result, when RRR is above 500, $Q_0(20K)$ becomes approximately constant under anomalous skin effect conditions.

The saturation of $Q_0(20K)$ is considered to occur as follows. When DC conductivity increases, the surface resistance decreases so that the surface electrons generated by the electric field are scattered in the skin depth and contribute to electrical conduction near room temperature where the mean free path of the electron is shorter than the skin depth. In extremely low temperatures, by the anomalous skin effect, the mean free path of surface electrons generated by the electric field is much longer than skin depth. Therefore some surface electrons propagate to the bulk. For this reason, the number of electrons contributing to the surface electric current is gradually saturated if the mean free path of the surface electron becomes long. As a

result, when DC conductivity becomes higher, the surface resistance decreases and becomes approximately constant. As shown in (1), RRR is proportional to the DC conductivity at extreme temperatures, and Q_0 is inversely proportional to the surface resistivity in extremely low temperatures. Thus, Q_0 is gradually saturated with increasing RRR under anomalous skin effect conditions, as shown in Figure 4.

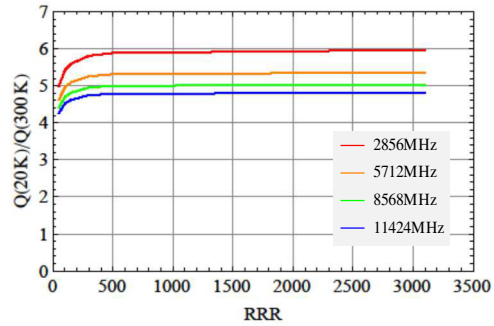


Figure 4: Relation between $Q_0(20K)/Q_0(300K)$ and RRR.

MEASUREMENT OF RRR AND Q_0

Measurement of RRR

We first measured the RRR value of high-purity copper as a cavity material. Then we obtained the relation between RRR and Q_0 by measuring Q_0 for a pillbox cavity made of 6N8 copper and of oxygen-free copper (Class 1) in the temperature range from 20 K to 300 K. We obtained the measurement data of RRR by (1) using DC resistivity (ρ). We measured ρ for 6N8 copper and Class 1 samples using the delta mode using a combination of a low voltage source meter, a nano volt meter and the four-terminal method. We determine that a sample size of $1 \times 1 \times 100$ mm and a current of 1A was required to obtain sufficient measurement sensitivity of voltage for samples of RRR10,000 in extremely low temperatures. We prepared the 6N8 copper and Class 1 samples by annealing at temperatures of 300, 500, 700, 900°C, and as grown. Figure 5 shows the annealed temperature dependence for the ratio of the DC resistivity at 300 K and 20 K. Figure 5 shows that the maximum of $\rho(300K)/\rho(20K)$ for Class 1 is about 300 and that of 6N8 copper is about 1500 at an annealing temperature of 700°C. The $\rho(300K)/\rho(20K)$ value seems to increase

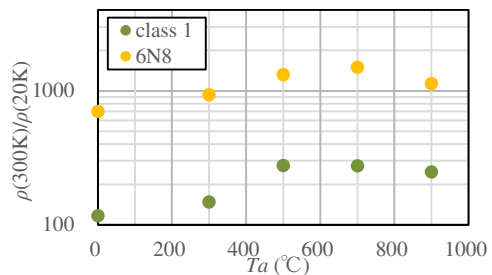


Figure 5: Relation between $\rho(300K)/\rho(20K)$ and the annealing temperature.

with stress relief by annealing, but when the annealing temperature is too high, the stress relief decreases as a result of brittle grain-boundary fracture.

Measurement of Q_0

We measured the Q_0 value for a pillbox cavity of the same dimensions as calculation parameters. The cavity is joined by gold brazing with a brazing temperature of approximately 900°C. Figure 6 shows the measurement results of the Q_0 ratio $\{Q_0(20K)/Q_0(300K)\}$ for cavities of Class 1 and 6N8 copper. Figure 7 shows the relation between $Q_0(20K)/Q_0(300K)$ and RRR. $Q_0(20K)/Q_0(300K)$ value of 6N8 copper is 5.2 and that of Class 1 is 4.8. These measurement values are lower than the calculation values by a few percent. From the results of the calculation and measurement, $Q_0(20K)/Q_0(300K)$ becomes high so that the purity of cavity is high, but $Q_0(20K)/Q_0(300K)$ is gradually saturated.

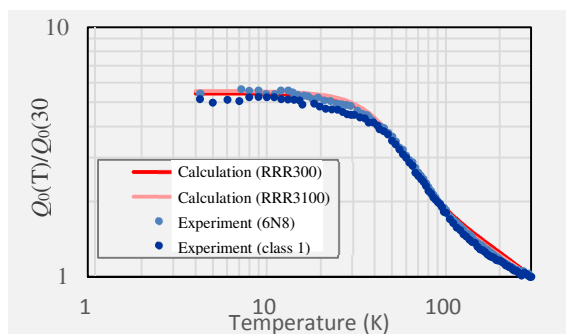


Figure 6: Relation between $Q_0(T)/Q_0(300K)$ and the temperature.

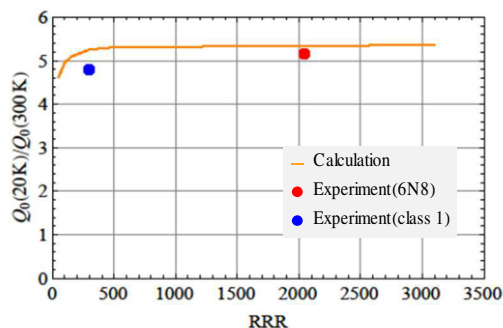


Figure 7: A agreement between the experimental results and calculation values of $Q_0(20K)/Q_0(300K)$.

LOW-POWER TEST OF THE ACCELERATING STRUCTURE

We measure the low-temperature RF characteristics for the accelerating structure which is made of 6N8 copper and is joined by diffusion bonding. The accelerating structure during low-power test at room temperature is shown in Figure 8, and the cryostat for cooling the accelerating structure is shown in Figure 9. The accelerating structure could not be cooled below 48.8 K. However, the corresponding values at 20 K are sufficient to proceed to the high-power test.

We are examining whether we should attach a super insulator to the waveguide of the heat flux source in the cryostat and add more refrigerators to increase the cooling effect.



Figure 8: The accelerating structure during low-power test at room temperature.



Figure 9: The cryostat for cooling the accelerating structure.

CONCLUSION

We demonstrated through calculation and measurement that Q_0 becomes approximately constant by the anomalous skin effect when RRR is greater than 500. Moreover, $Q_0(20K)/Q_0(300K)$ of a C-band pillbox cavity made of 6N8 copper is not much greater than that of Class 1 copper, and $Q_0(20K)/Q_0(300K)$ becomes saturated. From the results of the DC resistivity measurement, because $\rho(300K)/\rho(20K)$ reaches a maximum value when the annealing temperature is about 700°C, a cavity annealed at about 700°C has the highest Q_0 value at extremely low temperatures. We plan to perform high-power tests of this accelerating structure at low temperatures in the future.

ACKNOWLEDGMENT

The authors would like to thank T. Shintomi (KEK) for his support of the low-power test stand constructing.

REFERENCES

- [1] I. Sato et al., “Developments of Coherent X-ray source based in cryogenic electron Linac”, in *Proc. 11th Int. Annual Meeting of Particle Accelerator Society of Japan (PASJ'14)*, Aomori, Japan, Aug. 2014, paper MOOL01, pp.176.
- [2] G. E. H. Reuter and E. H. Sondheimer, *Proc. R. Soc. London*, A195, 336 (1948).
- [3] W. Weingarten, “CAS RF engineering for particle accelerators”, CERN, Geneva, Switzerland, Rep. CERN-92-03, June 1992, pp. 318.